Materials Sciences and Applications, **2010, 1, 336-342**
doi:10.4236/msa.2010.16049 Published Online December 2010 (http://www.scirp.org/journal/msa)

Scientific Research

Characteristic and Performance of Elementary Hemp Fibre

Dasong Dai, Mizi Fan

Civil Engineering Department, School of Engineering and Design, Brunel University, London, UK.
E-mail: mizi.fan@brunel.ac.uk

Received September 6th, 2010; revised November 16th, 2010; accepted November 20th, 2010.

ABSTRACT

This paper presents systematic and improved methodologies to characterize the surface and fracture of elementary hemp fibres by Field Emission Scanning Microscope (*FE-SEM*)*, determine the Microfibril Angles* (*MFA*) *by an advanced microscopy technology and examine the crystallinity by X-Ray Diffraction* (*XRD*) *and Fourier Transform Infrared* (*FTIR*)*. The results showed that* 1) *There existed various deformations/defects in elementary hemp fibres, showing four types of deformations, namely kink bands, dislocations, nodes and slip planes. The crack on the surface of elementary fibres was the initial breaking point under stress;* 2) *Under tension the primary wall and secondary wall of hemp fibres showed different deformation and breaking behaviour. The crack initiated in a weak point of primary wall and subsequently propagated along radial direction from S*1 *to S*2 *layers;* 3) *The average MFA for the broken regions of S*2 *layer was* 6.16˚ *compared to* 2.65˚ *for the normal hemp fibres and the breaking of hemp fibres occurred at the points where had the biggest MFA;* 4) *The average MFA was* 2.65˚ *for S*2 *layer and* 80.35˚ *for S*1 *layer;* 5) *The Crystallinity Index* (*CI*) *determined by XRD and FTIR was very similar, showing the lattice parameters of the hemp fibres tested a =* 6.97 *Å, b =* 6.26 *Å, c =* 11.88 *Å and γ =* 97.21˚*, and the ratio of* 1423 *to* 896 cm^{-1} *was found more suitable for CI evaluation for hemp fibres.*

Keywords: *Natural Fibres, Fracture, Crack, X-Ray Diffraction* (*XRD*)*, Fourier Transform Infrared Spectroscopy* (*FTIR*)

1. Introduction

Hemp fibre has widely been used in many civilizations. It has been reported that the earliest use of hemp was over 6000 years ago [1-3]. The increasing environmental awareness, growing global waste problems and continuously rising high crude oil prices have motivated governments all over the world to increase the legislative pressure. This in turn promotes researchers, industries and farmers to develop the concepts of environmental sustainability and reconsider renewable resources. Renewable resources from agricultural or forestry products form a basis for new industrial products or alternative energy sources, such as hemp fibre [4]. Hemp fibres have long been valued for their high strength and long fibre length, and used extensively in the fabrication of ropes and sails, as well as for paper and textiles. Hemp fibres consist of different hierarchical microstructures, whereby microfibrils serve as basic units. The microfibrils are embedded in a matrix of hemicelluloses and form the different cell wall layers of an elementary fibre, which generally has a large average diameter ranging from 10 to 50 m [5]. The elementary fibres are bonded together with pectin's and small amounts of lignin framing the next level of microstructure, *i.e.* technical fibres, with a diameters ranging from 50 to 100 m [6]. These filaments are fixed together with a pectin-lignin matrix to form fibre bundles in the cortex of plant stems. Thus, bast fibres are bundles of individual strands of fibres held together by a pectin-lignin interface [7].

The fibres of never dried hemp contain numerous deformations. All these deformations appear where there is a change in microfibril direction and a distorsion of the fibrils. The deformations can be seen under polarized light [8-14], but the largest of them also could be discerned without polarisers [15] (e.g. SEM [16-18], Raman spectroscopy [19-22]). The deformation of fibres can affect the strain distribution in elementary fibre, leading to localized strain concentrations [23], and hence reduce both compressive strength and tensile strength [24], which was also proved by a finite element (FE) modeling

of the tensile behaviour of single flax and hemp fibre [25]. The fibres in the matrix may break at the point with deformations [26], and the concentration of stresses around the deformation could act as the site of initiation of fibre-matrix debonding as well as for the formation of micro-cracks in the matrix which contribute to global fracture of composite [27]. Limited work conducted on the breaking behaviour of wood pulp [28], cotton [29], and flax [30] also indicated that the break behaviour of the primary and secondary cell wall of the flax fibres was different from that of wood and cotton [17]. The primary cell wall generally breaks in a brittle manner, whereas the secondary cell wall, bridged by fibrils, splits relatively easily along the length direction.

The experience has highlighted that it is not possible to use or appropriate to compare data available from different investigations reported in the literatures. Measuring natural fibres proves to be a great challenge. Microstructural defects, fibre abstraction (e.g. single fibre) and processing are all yet to be studied. This paper is an attempt to characterize the surface and reveal the failure mechanism of elementary hemp fibres. Systematic and improved methodologies and advanced technologies have been developed to investigate the microfibril angles of elementary hemp fibres and the crystallinity of hemp fibres. The surface of hemp fibres after tensile loading and fracture of fibres after breaking were also observed carefully to characterize the surface and reveal the failure mechanism of elementary hemp fibres. This paper is the first of a series of papers from an intensive research programme aiming at a better understanding of natural fibre resources and the development of their high strength composites for applications in various industrial sectors.

2. Materials and Methods

2.1. Materials

Hemp fibres were supplied by a Hemp Farm & Fibre Company Ltd, UK. The fibres arrived in a form of fibre bundles. Salt products, namely, copper (II) nitrate (30 wt %) and cobalt (II) chloride (≥ 98.0%) were obtained from Sigma-Aldrich Company Ltd, UK.

2.2. Microfibril Angle (MFA) Measurement

Hemp fibres (0.1 g) were placed into a beaker contained 100 ml salt solution (5%, wt/vol), whether copper nitrate or cobalt chloride, and heated at 80˚C for 2 hours. The beaker container was placed into ultrasonic bath and treated at 80˚C for 2 hours. The treated hemp fibres were finally washed with distill water. Photomicrographs were taken using BX51 Reflected Light Microscope equipped with a CAM-XC50-5MP cooled CCD camera, then using UTHSCSA ImageTool to measure the microfibril angle of S1 and S2 layers. 50 test pieces were used.

2.3. Deformation of Hemp Fibres

Optical microscopy was employed to examine the deformation of hemp fibres. The BX51 Reflected Light Microscope equips with 5 ×, 20 ×, 50 ×, 100 × objectives, a CAM-XC50-5MP cooled CCD camera and 100 W Halogen for transmitted or reflected light. The fibres were positioned on a slide using cyanacrylate glue and covered with a cover slip. Images were analysed and captured as 2576 × 1932 RGB jpeg files. The experiments were performed at room temperature and 1000 test pieces were examined.

2.4. Fracture Characterization

Surface and fracture characterization of hemp fibres were conducted within a Zeiss Supra 35 VP field emission scanning electron microscope (FE-SEM). Individual fibres were randomly and gently isolated from fibre bundles. The isolated fibres were conditioned at 20 ± 2˚C and 65 ± 2% relative humidity before temporarily fixed on the mounting card (**Figure 1**) with adhesive tape. A droplet of glue was applied on the centre of both sides of the hole along the length of card. The testing was then carried out as fellows:

1) Subject the prepared samples to SEM and characterize the surface of the test pieces;
2) Subject the samples to tensile strength test by using Instron 5566 at a crosshead speed of 0.1 mm/min and with 10 mm gauge length. The test results of mechanical performance of the elementary fibres are presented in a separate paper (Dai, *et al*. 2010);
3) Re-sample the test pieces for fracture characterization from the broken test pieces after tensile tests and subject them to oven-drying at 105˚C. The test pieces were then coated with a thin layer of platinum in an

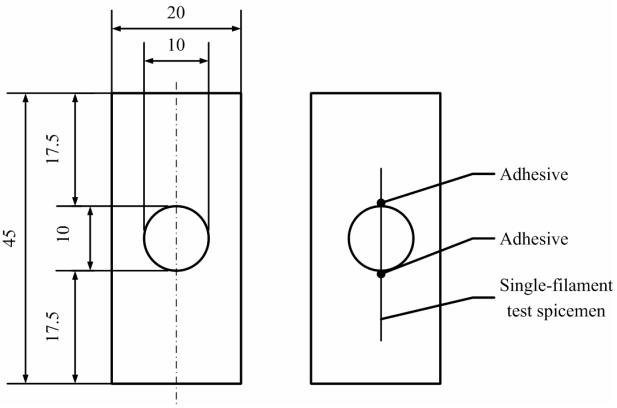

Figure 1. Set-up of single fibre testing: a = specimen mount, b = test specimen mounted on the mount.

Edwards S150B sputter coater (BOC Edwards, Wilmington, MA) to provide electrical conductivity. The fracture surface of the coated test pieces were observed by using the secondary electron mode images (digitally). 50 test pieces were used.

2.5. Crystallinity of Hemp Fibres

The crystallinity of hemp fibres was determined by using a powder X-Ray Diffraction Method (PXRD). A D8 advanced Bruker AXS diffractometer, Cu point focus source, graphite monochromator and 2D-area detector GADDS system were used. The diffracted intensity of CuKα radiation (wavelength of 0.1542 nm) was recorded between 5˚ and 60˚ (2θ angle range) at 40 kV and 40 mA. Samples were analyzed in transmission mode. The unit cell of hemp fibre was calculated by DIFFRAC ^{plus} software, and the Crystallinity Index (CI) was evaluated by using Segal empirical method [30] as follows:

$$CI\% = \frac{(I_{002} - I_{am})}{I_{002}} \times 100\% \quad (1)$$

where I_{002} is the maximum intensity of diffraction of the (002) lattice peak at a 2θ angle of between 22˚ and 23˚, which represents both crystalline and amorphous materials. And I_{am} is the intensity of diffraction of the amorphous material, which is taken at a 2θ angle between 18˚ and 19˚ where the intensity is at a minimum [31]. It should be noted that the crystallinity index is useful only on a comparison basis as it is used to indicate the order of crystallinity rather than the crystallinity of crystalline regions. 100 replicates were used.

2.6. Composition of Hemp Fibres

Composition of hemp fibres was examined by using Fourier Transform Infrared Spectroscopy (FTIR) measurement which uses a Perking-Elmer spectrometer and the standard KBr pellet technique. A total of 16 scans were taken for the sample between 650 cm^{-1} and 4000 cm^{-1}, with a resolution of 2 cm^{-1}. Hemp fibres were ground and mixed with KBr and then pressed into a pellet for FTIR measurement.

3. Results and Discussion

3.1. Microfibril Angle (MFA) of Hemp Fibres

The orientations of hemp fibres treated with both copper (II) nitrate and cobalt (II) chloride solutions can be detected under light microscope. However, it was found that the orientations of MFA in the samples treated with the former solution were much more distinctive than those with the latter solution treatment. This may result in more accurate measurements of MFA. An example of microfibril orientations in S1 and S2 layers observed under light microscope at 1000 × is given in **Figures 2(a)** and **2(b)**. It was found that, microfibrils in S2 layer have a Z-helical orientation, while in S1 layer have S-helical orientation. The average MFA in S2 inner layer is 2.65˚ (arrange from 1˚ to 3.27˚), which is smaller than 4˚ measured previously by Fink [32]. This may be due partly to the different hemp fibres from different geographical sources. The average MFA in the outer part of S2 layer ranges from 23˚ to 30˚. The average MFA in S1 layer is 80.35˚ (range from 77.7˚ to 86.2˚), which is in agreement with the results of previous worker [33] who found the average angle in S1 layer was 70-90˚.

3.2. Crystal Structure of Hemp Fibres

X-ray crystallography was used to investigate the crystallinity of hemp fibres. An example of X-ray powder diffraction photograph from hemp fibres is given in **Figure 3**. It can be seen from **Figure 3** that the major crystalline peak of the hemp fibres occurred at 2θ = 22.1˚, which represents the cellulose crystallographic plane (002, Bragg reflection). The minimum intensity between 002 and 110 peaks (I_{am}) is at 2θ = 18.6˚. The crystallinity

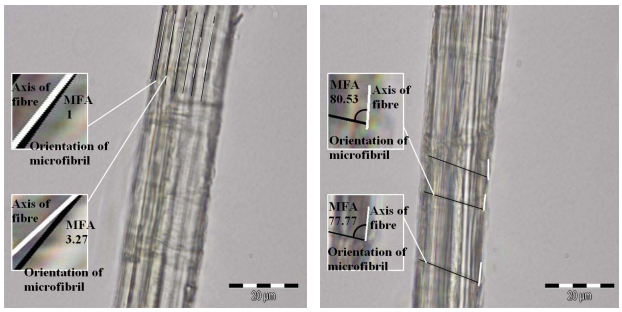

(a) (b)

Figure 2. Microfibril angle of hemp fibre: MFA in S2 layer (a); MFA in S1 layer (b).

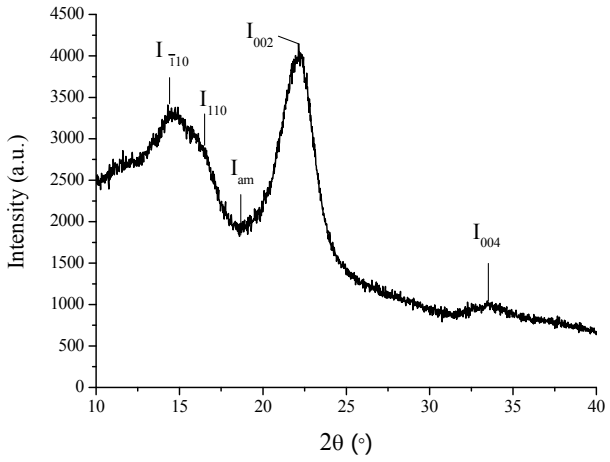

Figure 3. X-ray diffractogram of hemp fibres.

index of hemp fibre is 56%. Other well-defined peaks present on the X-ray diffractogram are at 2θ = 14.3˚, 2θ = 16.8˚ and 2θ = 32.3˚, and these reflections correspond with the (110), (110) and (004) crystallographic planes, respectively. The lattice parameters of hemp fibres which were calculated by DIFFRAC ^{plus} are: a: 6.97 Å; b: 6.26 Å; c: 11.88 Å; γ: 97.21˚.

3.3. FTIR Analysis

Infrared spectrum of hemp fibres is displayed in **Figure 4**. The typical functional groups and the IR signal with the possible sources are listed in **Table 1** for a reference. It could be observed from **Table 1** that five components exist in the hemp fibres after retting pretreatment. **Figure 4** shows a weak absorbance around 1729 cm^{-1} in the FTIR spectrum of hemp fibre, which might be attributed to the presence of the carboxylic ester (C=O) in pectin and waxes. Intensities of some bands in IR spectra have been found to be sensitive to variations of cellulose crystallinity and have been used to evaluate Crystallinity Index (CI) of cellulose. The ratios of peaks at 1423 cm^{-1} and 896 cm^{-1}, 1368 cm^{-1} and 2887 cm^{-1} and 1368 cm^{-1} and 662 cm^{-1} are normally used to measure CI e.g. [34-37]. In this study, the ratio of 1368 cm^{-1} and 2887 cm^{-1} is above 1 which seems to be unsuitable for evaluation, while the ratios of 1423 to 896 cm^{-1} and 1368 to 662 cm^{-1} are 55.7% and 49.3% respectively. The value calculated by using Segal empirical method is 56%, indicating that the ratio of 1423 to 896 cm^{-1} is more suitable for CI evaluation.

3.4. Deformation of Hemp Fibres

Optical microscope observation showed that much deformation has occurred in hemp fibres and some types of deformation are difficult to distinguish. In this study, any defect of fibres which may affect the mechanical properties of the fibres, especially the tensile strength, was recorded and called deformation. The results of numerous examinations (1000 test pieces) of hemp fibres can be cataloged into four types of deformation of hemp fibres (**Figure 5**). The characteristic of each type deformation are as follows: 1) Kind bands, formed in the fibres as a result of axial curing stresses; 2) Nodes, formed in the regions of localized delamination and compressive strain; 3) Dislocations, appeared in untreated natural fibre; and 4) Slip planes, crinkled in the cell wall resulting from a slight linear displacement of the wall lamellae. It is apparent that these deformations appear when there is a change in microfibril direction and a distorsion of fibrils.

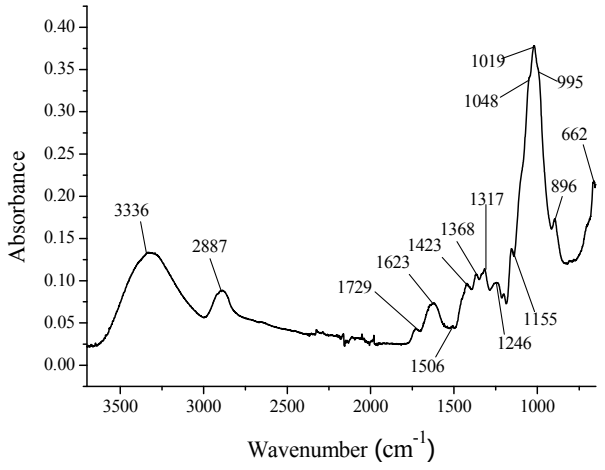

Figure 4. FTIR spectra of hemp fibres.

Table 1. Main infrared transition for hemp fibre.

Wavenumber (cm^{-1})	Vibration	Sources
3336	OH stretching	Cellulose, Hemicellulose
2887	C–H symmetrical stretching	Cellulose, Hemicellulose
1729	C=O stretching vibration	Pectin, Waxes
1623	OH bending of absorbed water	Water
1506	C=C aromatic symmetrical stretching	Lignin
1423	HCH and OCH in-plane bending vibration	Cellulose
1368, 1362	In-the-plane CH bending	Cellulose, Hemicellulose
1317	CH2 rocking vibration	Cellulose
1246	C=O and G ring stretching	Lignin
1202	C-O-C symmetric stretching	Cellulose, Hemicellulose
1155	C-O-C asymmetrical stretching	Cellulose, Hemicellulose
1048, 1019, 995	C-C, C-OH, C-H ring and side group vibrations	Cellulose, Hemicellulose
896	COC,CCO and CCH deformation and stretching	Cellulose
662	C-OH out-of-plane bending	Cellulose

Nevertheless, whilst it is clear that some of deformations occur during plant growth, a significant amount of deformation is resulted from decortication and other down-line processing. Deformations could be the weak points which broken at beating, mechanical treatment and in acidic environments. It is believed that stress concentrations around deformations can act as sites for the initiation of fibre matrix debonding as well as for the formation of micro cracks in the matrix.

3.5. Breaking Process

Figures 6(a-c) illustrate the initial and final fracture of an elementary hemp fibre. It was found that the

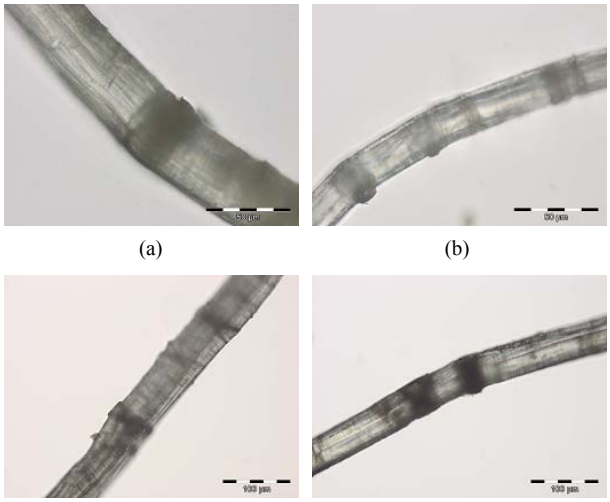

(a) (b) (c) (d)

Figure 5. Deformation of hemp fibre: a = kink band (× 500 magnification), b = node (× 500 magnification), c = dislocation (× 200 magnification), d = slip plane (× 200 magnification).

initial crack of hemp fibres starts from primary wall (**Figure 6(a)**). This may be due partly to the fact that the primary cell wall could contain a large fraction of amorphous pectin, hemicelluloses, cross-linked lignin and randomly oriented cellulose as reported previously [38-40]. The crack then proceeds into the secondary cell wall (S2) which forms the major part of hemp fibre. While the S2 layer has been reported containing several layers [41], this study showed that it at least contains the outer and inner parts of S2 layers and the MFA of which gradually decreases. The S2 layer consists of highly crystalline (CI 60%) cellulose microfibrils (**Figure 4**) bounded together by lignin and hemicellulose. The microfibrils are oriented spirally around the fibre axis. In this study, the microfibrils in the inner part of S2 layer have an MFA of about 2.65˚ with respect to the fibre axis, which explains the stiffness and strength of the fibre in the axial direction. The MFA in the outer part of S2 layer ranges from 23˚ to 30˚. The microfibril angle can strongly influence mechanical properties of fibres, such as tensile strength and modulus [42], which decrease with MFA increases. This means that the strength of inner part of S2 layer shall be higher than that of the outer part of S2 layers. Therefore, the breaking process in secondary wall of hemp fibres is from S1 layer to outer part of S2 layer to inner part of S2 layer (**Figures 6(b,c)**).

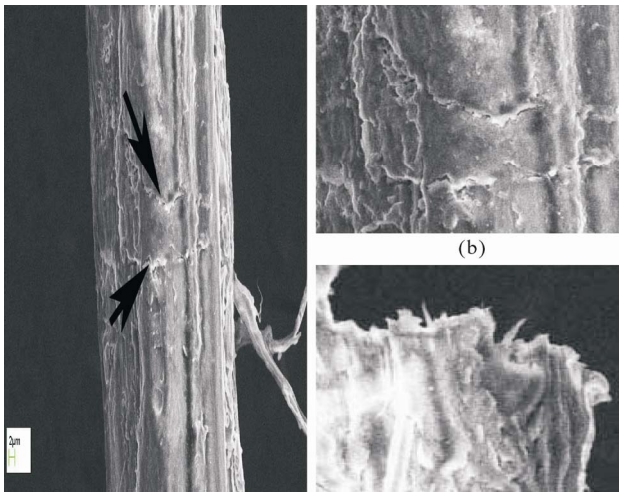

(a) (b) (c)

Figure 6. Breaking process under tension: Initial crack (a, b), fracture (c) of hemp fibre.

3.6. Fracture of Hemp Fibres

Figure 7 shows the fractography of hemp fibres. The macrofibril can be observed clearly in the fracture surface of hemp fibres. The MFA in the S2 layer at fracture point was measured and their mean value is 6.16˚ with respect to the fibre axis. As discussed in the previous sections, the average MFA in the S2 layer of non-defect hemp fibre is 2.65˚, indicating that the microfibril direction changes in the fracture regions of fibre. According to Mohlin *et al*. [43], the deformations, which change the direction of the fibre axis, have a negative influence on mechanical properties of fibre. Baley [14] reported that cracks in the flax fibre firstly happened in the area of kind band. However, the different strength between the different types of deformation as defined in this study have not been observed, although it was evident that the deformation is the main cause for the break of hemp fibres, that is, deformation is the weak link in hemp fibres.

4. Conclusions

A systematic and comprehensive study on the characteristic and behaviour of elementary hemp fibres presented in the paper concluded that:

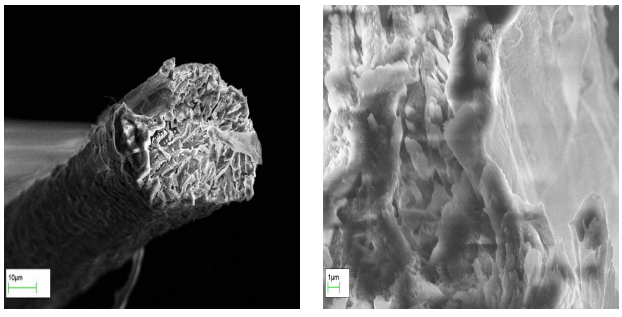

(a) (b)

Figure 7. Fractography of hemp fibre: a = overall view, b = detail of single fiber fracture.

1) An improved, accurate method of measure Microfibril Angle (MFA) of elementary hemp fibres could be developed (in this study): The average MFA was 2.65˚ for S2 layer and 80.35˚ for S1 layer. It was observed that the type of solutions had an influence on the effectiveness of pre-treatment which may had an implication of accuracy of measurement. The solution of $Cu(NO_3)_2$ was found more effective than $CoCl_2$.

2) The lattice parameters of hemp fibre studied were a = 6.97Å, b = 6.26 Å, c = 11.88 Å and γ = 97.21˚. The Crystallinity Index (CI) determined by XRD and FTIR was very similar, and the ratio of 1423 to 896 cm^{-1} was found more suitable for CI evaluation for hemp fibres.

3) The characterization on the surface of hemp fibres after tensile testing and the fracture of the broken fibres showed that there existed various deformations in elementary hemp fibres. However, the deformation of hemp fibres could be cataloged into four types, namely kink bands, dislocations, nodes and slip planes.

4) Under tensile stress, the initial crack was mainly from the primary wall and the crack proceeded into the secondary wall of hemp fibre, giving a breaking order of S1 layer to out part of S2 layer to inner layer of S2 layer. The average MFA (6.16˚) at the fracture points of the S2 layer was much higher than that of normal fibres (2.65˚).

5. Acknowledgements

This research programme is funded by the Technology Strategy Board, Department for Business, Innovation and Skills, UK.

REFERENCES

[1] J. W. Roulac, "Hemp Horizons: The Comeback of the World's Most Promising Plant," Chelsea Green Publishing Co., White River Junction, 1997.

[2] G. Beckermann, "Performance of Hemp-Fibre Reinforced Polypropylene Composite Materials," Waikato University, Hamilton, 2007.

[3] P. G. Stafford and J. Bigwood, "Psychedelics Encyclopedia. Berkeley, California," Ronin Publishing, Inc, Oakland, 1992.

[4] B. B. Jungbauernschaft, "Biomasse-Nachwachsende Rohstoffe," In: Fakten & Trends 2002 Zur Situation der Landwitschaft, Eggenfelden, 2002, pp. 191-207.

[5] M. D. Candilo, P. Ranalli, C. Bozzi and B. Focher, "Preliminary Results of Tests Facing with the Controlled Retting of Hemp," *Industrial Crops and Products*, Vol. 11, No. 2, 2001, pp. 197-203.

[6] B. M. Prasad and M. M. Sain, "Mechanical Properties of Thermally Treated Hemp Fibres in Inert Atmosphere for Potential Composite Reinforcement," *Materials Research Innovation*, Vol. 7, No. 4, 2003, pp. 231-238.

[7] H. J. Purz, H. P. Fink and H. Graf, "The Structure of Natural Cellulosic Fibres. Part I: The Structure of Bast Fibres and Their Changes by Scouring and Mercerization as Revealed by Optical and Electron Microscopy," *Das Papier*, Vol. 6, No. 52, 1998, pp. 315-324.

[8] R. P. Kibblewhite, "Fractures and Dislocations in the Walls of Kraft and Bisulphite Pulp Fibres," *Cellulose Chemistry Technology*, Vol. 10, No. 4, 1976, pp. 297-503.

[9] P. Hoffmeyer, "Non-Linear Creep Caused by Slip Plane Formation," *Wood Science Technology*, Vol. 27, No. 5, 1993, pp. 321-335.

[10] U. B. Mohlin, J. Dahlbom and J. Hornatowska, "Fibre Deformation and Sheet Strength," *Journal of Tappi*, Vol. 79, No. 6, 1996, pp. 105-111.

[11] M. J. Ellis, G. G. Duffy, R. W. Allison and R. P. Kibblewhite, "Fibre Deformation During Medium Consistency Mixing: Role of Residence Time and Impeller Geometry," *Appita Journal*, Vol. 51, No. 1, 1998, pp. 643-649.

[12] R. W. Allison, M. J. Ellis and R. P. Kibblewhite, "Effect of Mechanical Processes on the Strength of Oxygen Delignified Kraft Pulp," *Proceedings of the 1998 International Pulp Bleaching Conference*, Helsinki,, 1998, pp. 159-166.

[13] C. H. Ljungqvist, R. Lyng and F. Thuvander, "Influence of Observable Damage on Spruce Latewood Pulp Fibre Properties," *Sustainable Natural and Polymeric Composites-Science and Technology, Proceedings from the* 23*rd Risø International Symposium on Materials Science*, 2002, pp. 231-238.

[14] C. Baley, "Influence of Kink Bands on the Tensile Strength of Flax Fibres," *Journal of Materials Science*, Vol. 39, No. 1, 2004, pp. 331-334.

[15] J. Andersons, E. Sparnins and E. PoriKe, "Strength Distribution of Elementary Flax Fibres for Composite Reinforcement," 11*th Int. Inorgantic-Bonded Fibre Composites Conference,* Madrid, 2008.

[16] H. L. Bos, Van den Oever MJA and O. C. J. J. Peters, "The Influence of Fibre Structure and Deformation on the Fracture Behaviour of Flax Fibre Reinforced Composites," *Proceedings of the 4th International Conference on Deformation and Fracture of Composites*, Manchester, 1997, pp. 499-504.

[17] H. L. BOS and A. M. Donald, "*In Situ* ESEM Study of the Deformation of Elementary Flax Fibres," *Journal of Materials Sciences*, Vol. 34, No. 13, 1999, pp. 3029-3034.

[18] L. G. Thygesen, J. B. Bilde-Sørensen and P. Hoffmeyer, "Visualisation of Dislocations in Hemp Fibres: A Comparison between Scanning Electron Microscopy (SEM) and Polarized Light Microscopy (PLM)," *Industrial Crops and Products*, Vol. 24, No. 2, 2006, pp. 181-185.

[19] W. Y. Hamad and S. J. Eichhorn, "Deformation Micromechanics of Cellulose Fibres," *Journal of Engineering Materials and Technology*, Vol. 119, No. 3, 1997, pp. 309-313.

[20] S. J. Eichhorn, R. J. Young and W. Y. Yeh, "Deformation Processes in Regenerated Cellulose Fibres," *Textile Research Journal*, Vol. 71, No. 2, 2001, pp. 121-129.

[21] S. J. Eichhorn, "Strain Induced Raman Shifts in the Spec-

tra of Natural Cellulose Fibres," *Journal of Materials Science Letters*, Vol. 19, No. 3, 2000. pp. 721-723.

[22] S. K. Kovur, K. Schenzel and W. Diepenbrock, "Orientation Dependent FT Raman Microspectroscopy on Hemp Fibres," *Macromolecular Symposia*, Vol. 265, No. 1, 2008, pp. 205-210.

[23] L. Mott, S. M. Shaler and L. H. Groom, "A Technique to Measure Strain Distributions in Single Wood Pulp Fibres," *Wood and Fibre Science*, Vol. 28, No. 4, 1996, pp. 439-437.

[24] J. H. Greenwood and P. G. Rose, "Compressive Behaviour of Kevlar 49 Fibres and Composites," *Journal of Materials Science*, Vol. 9, No. 11, 1974, pp. 1809-1814.

[25] T. Nilsson and P. J. Gustafsson, "Influence of Dislocations and Plasticity on the Tensile Behaviour of Flax and Hemp Fibres," *Composites Part A: Applied Science and Manufacturing*, Vol. 38, No. 7, 2007, pp. 1722-1728.

[26] B. Focher, "Physical Properties of Flax Fibre," In: H. S. Sharma and C. F. Sumere van, Eds., *The Biology and Processing of Flax*, M Publications, Belfast, 1992, p. 333.

[27] M. Hughes, G. Sebe and J. Hague, "Investigation into the Effects of Micro-Compressive Defects on Interphase Behaviour in Hemp-Epoxy Composites Using Half-Fringe Photoelasticity," *Composite Interfaces*, Vol. 7, No. 1, 2000, pp. 13-29.

[28] W. Y. Hamad, "Some Microrheological Aspects of Wood-Pulp Fibres Subjected to Fatigue Loading," *Cellulose*, Vol. 4, No. 1, pp. 51-56.

[29] H. E. Gram, "Durability of Natural Fibres in Concrete," Swedish Cement and Concrete Research Institute, 1983, pp. 225.

[30] L. Segal, J. J. Creely, A. E. Martin and C. M. Conrad., "An Empirical Method for Estimating the Degree of Crystallinity of Native Cellulose Using the X-Ray Diffractometer," *Textile Research Journal*, Vol. 29, No. 10, 1959, pp. 786-794.

[31] M. B. Roncero, A. L. Torres, J. F. Colom and T. Vidal, "The Effect of Xylanase on Lignocellulosic Components during the Bleaching of Wood Pulps," *Bioresource Technology*, Vol. 96, No. 1, 2005, pp. 21-30.

[32] H. P. Fink, E. Walenta and J. Kunze, "The Structure of Natural Cellulosic Fibres-Part 2. The Supermolecular Structure of Bast Fibres and Their Changes by Mercerization as Revealed by X-Ray Diffraction and ^{13}C-NMR-Spectroscopy," *Papier*, Vol. 53, No. 9, 1999, pp. 534-542.

[33] A. Thygesen, G. Daniel and H. Lilholt, "Hemp Fibre Microstructure and Use of Fungal Defibration to Obtain Fibres for Composite Materials," *Journal of Natural fibres*, Vol. 2, No. 4, 2006, pp. 19-37.

[34] Y. Kataoka and T. Kondo, "FT-IR Microscopic Analysis of Changing Cellulose Crystalline Structure during Wood Cell Wall Formation," *Macromolecules*, Vol. 31, No. 3, 1998, pp. 760-764.

[35] R. T. O'Connor, E. F. Dupre and D. Mitchman, "Applications of Infrared Absorption Spectroscopy to Investigations of Cotton and Modified Cottons," *Textile Research Journal*, Vol. 28, No. 5, 1958, pp. 382-392.

[36] L. Ferru and P. Page, "Water Retention Value and Degree of Crystallinity by Infrared Absorption Spectroscopy in Caustic Soda Treated Cotton," *Cellulose Chemistry and Technology*, Vol. 11, No. 3, 1977, pp. 633-637.

[37] M. L. Troedec, D. Sedan, C. Peyratout, J. P. Bonneta, A. Smitha, R. Guinebretiereb, V. Gloaguenc and P. Krauszc, "Influence of Various Chemical Treatments on the Composition and Structure of Hemp Fibres," *Composites Part A*: *Applied Science and Manufacturing*, Vol. 39, No. 3, 2008, pp. 514-522.

[38] H. L. Bos, M. J. A. Van den Oever and O. C. J. J. Peters, "Tensile and Compressive Properties of Flax Fibres for Natural Fibre Reinforced Composites," *Journal of Materials Science*, Vol. 37, No. 8, 2002, pp. 1683-1692.

[39] K. Persson, "Modelling of Wood Properties by a Micromechanical Approach," Lund University, Lund, 1997.

[40] A. K. Bledzki and J. Gassan, "Composites Reinforced with Cellulose Based Fibres," *Progress in Polymer Science*, Vol. 24, No. 2, 1999, pp. 221-274.

[41] A. Thygesen, "Properties of Hemp Fibre Polymer Composites-An Optimization of Fibre Properties Using Novel Defibration Methods and Fibre Characterization," Royal Agricultural and Veterinary University of Denmark, Roskilde, 2006.

[42] E. C. Mclaughlin and R. A. Tait, "Fracture Mechanism of Plant Fibres," *Journal of Materials Science*, Vol. 15, No. 1, 1980, pp. 89-95.

[43] U. B. Mohlin and C. Alfredsson, "Fibre Deformation and Its Implications in Pulp Characterization," *Nordic Pulp and Paper Research Journal*, Vol. 5, No. 4, 1990, pp. 172-179.

